DEUTSCHES ELEKTRONEN-SYNCHROTRON DESY

DESY 89-018
February 1989

Heavy Flavour Production in High Energy Electron-Proton Collisions
Theoretical Issues and Expectations at HERA and Beyond

G.A. Schuler
II. Inst. f. Theoretische Physik, Univ. Hamburg

ISSN 0418-9833

NOTKESTRASSE 85 · 2 HAMBURG 52

To be sure that your preprints are promptly included in the
HIGH ENERGY PHYSICS INDEX ,
send them to the following address (if possible by air mail) :

DESY
Bibliothek
Notkestrasse 85
2 Hamburg 52
Germany

DESY 89–018
February 1989

ISSN 0418–9833

Heavy Flavour Production in High Energy Electron-Proton Collisions

Theoretical Issues and Expectations at HERA and Beyond [1]

G. A. Schuler
II. Institut für Theoretische Physik,
Universität Hamburg

Abstract

I review the status of the theory of heavy quark production in ep collisions. The various production modes are discussed and cross-section estimates given. Uncertainties in the theoretical cross-section calculation are investigated. The characteristics of heavy quark production in ep collisions are outlined.

1 Introduction

I review the status of the theory of heavy quark production in ep collisions. Heavy flavour physics in ep collisions is first of all important for "practical" reasons like the interpretation of charged lepton signals, search for new heavy quarks, study of B physics or background estimates. For these reasons it is necessary to have a reliable description of heavy flavour events in ep collsisions. Boson gluon fusion into a heavy quark-antiquark pair is the dominant production mechanism and many characteristics of heavy flavour events can be understood in this model. Yet there is also the theoretical interest to aim a precise quantitative test of the parton approach and of the QCD predictions in a highly non-trivial dynamical situation. In this context it is important to discuss the various possibilities of heavy quark production in ep collisions as well as to critically examine the related theoretical sources of uncertainty. After having presented total production cross-sections in section 2 I deal with these problems in Section 3. The general characteristics of heavy flavour events in ep collisions are then outlined in Section 4.

[1] Invited talk at the 5^{th} Workshop of the INFN ELOISATRON PROJECT, Erice, Italy, June 10 – 17, 1988.

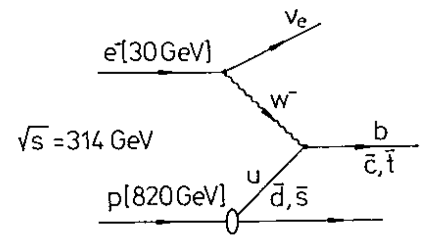

Figure 1: *Quark-Parton Model diagram contributing to the charged current interaction giving a single heavy quark.*

2 Total production cross-sections

In lepton-nucleon collisions, heavy quark production can already occur in the Quark-Parton Model (QPM) via the charged current process

$$e^{\pm}(l_e) + q(p) \rightarrow \nu(l') + Q(p_Q) \tag{1}$$

shown in Figure 1. Here the $W^{\pm}$ emitted from the incoming electron (positron) picks a light quark out of the proton and turns it into a heavy one resulting in a cross-section proportional to the square of the appropriate Cabbibo-Kobayashi-Maskawa (CKM) matrix element. It turns out that the tiny mixing angles between the light quarks and the heavy quarks cannot be compensated by the abundance of the former in the proton. In fact, the QPM contribution to heavy quark production is negligble compared to the other production mechanisms [1] making it extremely difficult to measure the CKM matrix elements of interest V_{cd}, V_{cs}, V_{td}, V_{ts}, V_{tb}, V_{cb}, V_{ub} at HERA through the CC processes (1). For a given cms energy $\sqrt{s}$ the cross-section for the QPM reaction (1) is specified by two kinematical variables, e.g. x and y, related to the boson momentum, $q = l_e - l'$, and the total hadronic energy, W, via the relations

$$Q^2 = -q^2 = xys \quad , \quad W^2 = (P+q)^2 = (1-x)ys. \tag{2}$$

Furthermore, x_q, the momentum fraction of the proton momentum, P, carried by the incoming quark equals Bjorken x, $x_q^{QPM} = x$.

In QCD the leading order contribution to heavy quark production is due to the $O(\alpha_s)$ boson-gluon fusion (BGF) mechanism shown in Figure 2.

$$V(q) + g(p) \rightarrow Q_f(p_f) + \bar{Q}_{f'}(p_{f'}). \tag{3}$$

In the charged current (CC) case V is the $W^{\pm}$ boson whereas in the neutral current (NC) case it corresponds to γ/Z^0 exchange and the produced quark and antiquark have the same flavour f. The cross-section

$$\sigma(e^{\pm}p \rightarrow Q\bar{Q}'X) = \int dy \int dQ^2 \int dx_g \int dz \int d\Phi\; g(x_g, \mu_F^2)\, h(y, Q^2, x_g, z, \Phi; \mu_R^2) \tag{4}$$

is a convolution of the gluon density $g(x_g, \mu_F^2)$ and a QCD part h for the subprocess. The latter [2] depends on the heavy quark masses, the electroweak charged/neutral

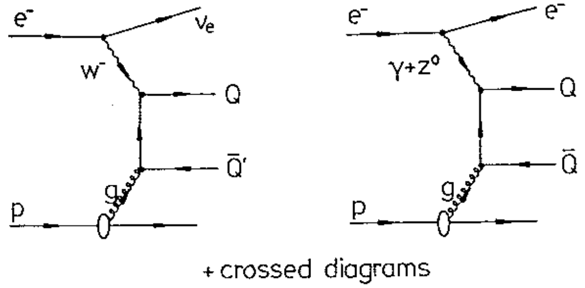

Figure 2: *Lowest order QCD diagrams for boson-gluon fusion into a heavy quark-antiquark pair.*

current structure including γ/Z^0 interference and polarization of the $e^{\pm}$ beam. The cross-section also depends on the two mass scales, the factorization mass in the gluon density, μ_F, and the renormalization mass in the strong coupling, μ_R. In addition to the normal deep inelastic scattering (DIS) variables (y, Q^2), three new independent variables enter: (i) the gluon momentum fraction x_g; (ii) the variable $z = P \cdot p_f / P \cdot q$ related to the angle θ between the $Q\bar{Q}$-axis and the boson-gluon axis in this subsystem cms (e.g. in the NC case we have: $2z = 1 - \beta\cos\theta$ where $\beta = \sqrt{1 - 4m^2/\hat{s}}$); and (iii) the azimuthal angle Φ between the lepton and hadron planes. I note that the gluon momentum fraction, x_g, is now related to the usual DIS variable x by

$$x_g = x + \frac{\hat{s}}{ys} \geq \max\left\{x, \frac{(m_f + m_{f'})^2}{s}\right\} \tag{5}$$

Here $\hat{s} = (p_f + p_{f'})^2$ is the invariant mass square of the $Q\bar{Q}'$ subsystem. Also, as opposed to the QPM subprocess (1), the BGF processes (3) need the gluon density in a proton as input. Thus ep colliders like HERA offer the possibility of extracting the gluon density by measuring specific heavy flavour distributions. To judge such prospects, however, a critical examination of the uncertainties in the cross-section calculation of eq. (4) is required. Also the possibilities of heavy quark production besides the BGF mechanism have to be investigated. I shall return to these problems in the next section after having presented total production rates based on BGF.

The inclusive heavy quark cross-section, $\sigma_Q = 2\sigma(ep \to eQ\bar{Q}X) + \sum_{Q'}\sigma(ep \to \nu Q\bar{Q}'X)$, is given in Figure 3 in terms of the ep (or μp) cms energy $\sqrt{s}$. The results are based on the BGF cross-sections evaluated in the leading order, $O(\alpha_s)$, using $\mu_F = \mu_R = \hat{s}$, $\Lambda = 200\,\mathrm{MeV}$ and $n_f = 6$ in the one-loop formula for α_s, and the gluon density parametrization set 1 of [3]. The charm cross-section is also shown using the the softer MRS [4] alternative. The quark masses are taken as $m_c = 1.5\,\mathrm{GeV}$, $m_b = 5\,\mathrm{GeV}$ and the top quark mass varied between $m_t = 50$ and 100 GeV. Concentrating on the HERA configuration of 30 GeV electrons on 820 GeV protons, the charm and bottom cross-sections are comparable to (or larger than) those expected at SLC/LEP. On the contrary, at the HERA energy, $\sqrt{s} = 314\,\mathrm{GeV}$, top quark production is still at threshold, i.e. the top cross-section varies strongly with the top quark mass. E.g. we find $\sigma_t = 4.1$, 0.31, 0.05 pb for $m_t = 40$, 60, 80 GeV, respectively. With an integrated luminosity of 200 pb^{-1}, corresponding to ~1 year of running at HERA, one would

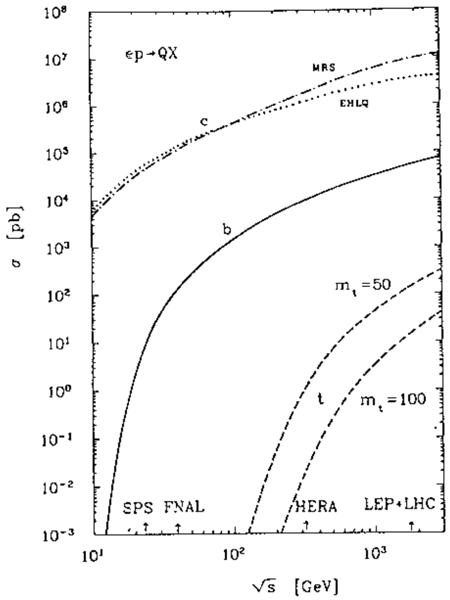

Figure 3: *Inclusive heavy flavour cross-section based on lowest order BGF. (EHLQ [3] gluon density, for charm also the softer MRS [4] alternative.)*

produce about 10^8 charm, a million bottom particles and still about 10 top events with $m_t = 80\,\mathrm{GeV}$ indicating the prospects of B physics at HERA (HERA a "bottom factory") and the limit up to which a top search at HERA seems to be feasible.

To understand the origin of these heavy quark cross-sections one has to distinguish between a light top ($m_t \leq 40\,\mathrm{GeV}$), charm and bottom on the one hand and a heavy top ($m_t > 55\,\mathrm{GeV}$) on the other hand. The large cross-sections in the former case are provided by neutral current processes at very low Q^2, i.e. γ exchange giving essentially real photoproduction. For a heavy top the CC process dominates due to the smaller threshold associated with single top quark production ($\bar{t}b$) in comparison to the pair production ($t\bar{t}$) in NC. Since heavy quarks with masses up to about 40 GeV are mainly photoproduced the Weizsäcker-Williams approximation (WWA) can be used to simplify their cross-section evaluation. Yet note that, as is the case for all leading approximations, there is some ambiguity on the choice of the upper and lower limits of Q^2. Thus the use of the WWA introduces an additional (unnecessary) uncertainty in the theoretical cross-section calculation.

I close this section by considering the contributions of heavy quark production to the DIS structure functions, $F_i(x, Q^2)$, in the NC and CC sectors,

$$F_i^{NC/CC} = F_i^{u,d,s} + F_i^c + F_i^b + F_i^t \tag{6}$$

Here u, d, s denotes the contributions from the light (massless) quarks. The structure

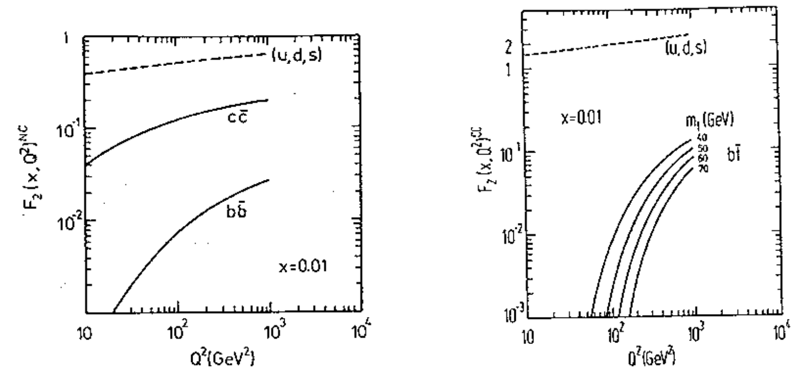

Figure 4: *Predicted Q^2 dependence of $F_2(x,Q^2)$ for NC events (a) and CC events (b) for $x = 0.01$ using $m_c = 1.3$ GeV and $m_b = 4.5$ GeV. The standard leading $\ln Q^2$ scaling violating contributions of the light quarks (u,d,s) to F_2 are shown by the dashed curves. The parton distributions are taken from [7].*

functions, $F_i^Q(x,Q^2)$, are defined in the usual way via [2,5,6]:

$$\frac{d^2\sigma^Q}{dxdy} = \frac{4\pi\alpha^2}{Q^2xy}\left\{g_1\left[xy^2F_1^Q(x,Q^2) + (1-y)F_2^Q(x,Q^2)\right] + g_2xy(2-y)F_3^Q(x,Q^2)\right\} \quad (7)$$

where $g_{1,2}$ are electroweak couplings suitable for the NC and CC case, respectively, which can be found e.g. in [2]. In the NC sector, Figure 4a [5], the $t\bar{t}$ contribution in the at HERA observable Q^2 range (given by $y \geq 0.01$) is unobservable small, less than 10^{-4}. The much larger $c\bar{c}$ component reaches its asymptotic leading logarithmic Q^2 dependence already at $Q^2 = 100\,\text{GeV}^2$, from there on the charm component of the proton behaves the same way ($\sim \ln Q^2$) as the light u, d and s quarks. This is clear since for $Q^2 \geq 4m_c^2$ only the logarithmic terms in the cross-section formula survive and we are left with the dominant $\ln Q^2$ terms as for massless quarks. For $b\bar{b}$ production, however, the powerlike-like m_b^2/Q^2 terms dominate over the whole Q^2 range accessible at HERA. But their absolute size is small as compared to the leading $\ln Q^2$ contributions from the light quarks. Thus it will be hard to observe a deviation from the logarithmic scaling violation due to the heavy quarks in the NC sector at HERA.

In the CC sector, Figure 4b [5], the contribution from top production ($\bar{t}b$) is sizeable at high values of Q^2 in the small x region. Since for kinematic reasons we are here close to the $\bar{t}b$ threshold, the top contributions strongly vary with Q^2 which gives rise to power-like deviations from the leading $\ln Q^2$ scaling violating terms due to all lighter quark contributions to F_i. The observation of such deviations from the logarithmic scaling violations could in principle be used as an indication for heavy quark (top) production. Yet, it turns out [5] that a resolution better than 5% would be needed which rules out this possibility. On the other hand, one can conclude that heavy quark production thresholds will not contaminate the leading $\ln Q^2$ scaling violation tests of QCD at HERA using $F_i(x,Q^2)$.

3 Uncertainties of the cross-sections

The total error on the heavy quark cross-sections is in part due to our ignorance of the different input quantities and in part to intrinsic theoretical ambiguities. Insufficient known input quantities are the heavy quark masses, the QCD scale Λ (and the number of flavours n_f), and the parton densities both inside the proton and inside the photon. Theoretical uncertainties arise from the choice of the renormalization and factorization mass scales, μ_R and μ_F. The effect of higher order terms should be included as well as the other channels of heavy quark production. Finally there is an ambiguity of attributing certain contributions as part of higher order QCD corrections to BGF or as resolved photon (see below) contributions.

A major source of uncertainty for charm and bottom production is the proper definition of the heavy quark masses (current or constituent) and the exact values to use. A decrease of these masses by 0.3 GeV from the assumed ones, $m_c = 1.5\,\text{GeV}$ and $m_b = 5.0\,\text{GeV}$, leads to an increase of the charm and bottom cross-sections by 68% and 22%, respectively, whereas an increase by 0.3 GeV gives a reduction by 36% and 17%, respectively.

Next there is an ambiguity due to our ignorance of the input structure functions. Yet there is a correlation between the value of Λ and the form of the gluon density in the QCD analysis of scaling violations in deep inelastic scattering. The extraction of the input gluon density and the subsequent QCD evolution have been performed using a definite value of Λ. Thus if one wants to change Λ, the parametrization of the gluon density must be chosen accordingly (or vice versa). I account for this fact by taking that value of Λ (and of n_f) that was used in the respective parametrization and estimate the resulting error by the use of different parametrizations [3,4,7,8]. Both the top and the bottom cross-sections are rather insensitive, they change by less than 25%. On the other hand, charm production is changed by up to a factor of two. The reason is not so much the change of α_s but the fact that charm production probes the gluon density, $g(x_g,\mu_F^2)$, down to $x_g \sim 10^{-4}$ where the gluon density is quite uncertain, whereas the range in x_g does not extend to such small values for top and bottom, see eq. (5).

Another important source of errors is introduced by the scale dependence of the result. In principle, one can distinguish the renormalization scale, μ_R, and the factorization scale, μ_F, c.f. eq. (4). On physical grounds the scales should be of the order of the heavy quark mass. In the following I identify the two scales and estimate the uncertainty in μ by varying it from half the heavy quark mass to twice its value, $m/2 \leq \mu \leq 2m$. The result is that the top cross-section increases by a factor two when lowering μ from $2m$ to $m/2$, whereas charm and bottom cross-sections are suprisingly stable. Depending on the respective parametrization of the gluon density they increase or decrease slightly by less than 20%. This last fact is due to an accidental cancellation in the lowest order BGF cross-section between the scale dependence of the gluon density and that of $\alpha_s(\mu)$. While the strong coupling constant increases as μ becomes smaller, the gluon density, $g(x_g,\mu)$, decreases if $x_g \leq 0.07$ as it is usually the case for charm and bottom production. For top production, on the other hand, $x_g \geq 0.07$, typically and thus the gluon density amplifies the increase of the cross-section through α_s as μ gets smaller.

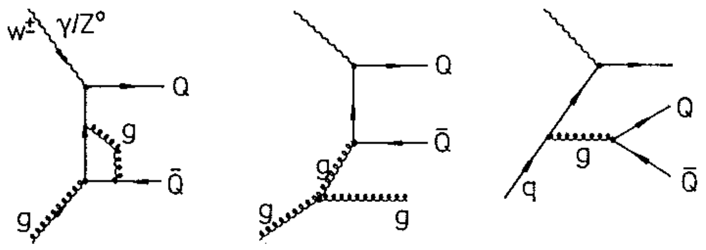

Figure 5: $O(\alpha_s^2)$ *diagrams contributing to heavy quark production in ep collisions.*

Based on the lowest order, $O(\alpha_s)$, alone it is not possible to rescue from the mass scale dependence, all values for μ are equally valid. A change of μ around m introduces an error of order $\alpha_s^2(m)$. At next-to-leading accuracy, the variation of μ in the leading term is automatically compensated at order α_s^2 by the corresponding change in the correction, so that the resulting error is in this case of order $\alpha_s^3(m)$. Thus, the ambiguity in the result for a given change of μ is normally decreased when going from the leading to the next-to-leading accuracy. This can of course not be expected for charm and bottom production due to the subtle cancellations of the mass scale dependences in these cases in the lowest order. A full $O(\alpha_s^2)$ calculation for ep collisions is still outstanding. It requires the calculations of diagrams shown in Figure 5 for nonzero Q^2. I use the result of the inclusive $O(\alpha_s^2)$ calculation of photoproduction of heavy quarks in [9] to estimate the next-to-leading effects in electroproduction using the WWA. In fact, the results I obtain are similar to those found for heavy quark production in $p\bar{p}$ collisions [10]. According to this approximation, top production increases by roughly a factor of two and becomes less sensitive to changes in μ with a maximum at $\mu \sim m/2$. Using the parton density parametrization set 1 of [3] (the one of [7]) the top cross-section varies between 1.8 pb and 2.6 pb (1.45 pb and 2.3 pb). Thus top production can be quite reliable computed. The maximum error due to changes in the parton densities and the mass scale is about 60%. On the other hand, bottom and charm cross-sections are more uncertain. Here $\sqrt{s}/m_Q$ is already so large that the corrective terms are dominant over the lowest order cross-section at all values of order m of the scale μ. The most important contributions to the cross-section come from the corrections to the BGF mechanism, in particular from the diagrams with a spin-1 gluon in the t-channel which dominate at the large values of $\sqrt{\hat{s}}/m_Q$ available at HERA for charm and bottom production. Since higher order corrections not only change the absolut normalization but also influence the event shape, a realistic event simulation should include these terms at least in an approximate way as it is e.g. done in [11].

Charm and bottom cross-sections are dominated by almost real photon exchange. Yet, at low Q^2 there are important contributions coming from subprocesses involving the photon structure function, see Figure 6. This latter which describes the quark and gluon content of the photon is given by the sum of a VDM component and of an anomalous component [12]:

$$p_{a/\gamma}(x,\mu^2) = p_{a/\gamma}^{VDM}(x,\mu^2) + p_{a/\gamma}^{AN}(x,\mu^2) \quad . \tag{8}$$

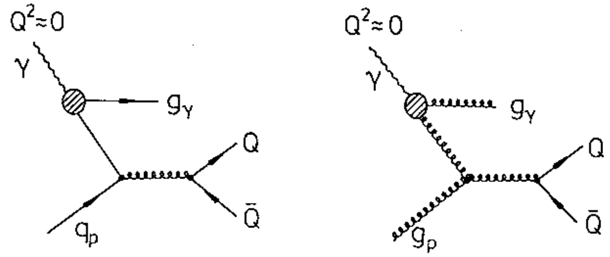

Figure 6: *Resolved photon contributions to heavy quark production in ep collisions.*

The anomalous component, proportional to $\log \mu^2/\Lambda^2$, is calculable in perturbarive QCD. The other one may be estimated using the VDM approach [13]. At higher values of the quark $p_\perp$ it is expected to be negligible. The anomalous component, in the following referred to as "resolved photon" contributions in contrast to the "direct" contribution through BGF, gives rise to gg and $q\bar{q}$ initiated hard scattering subprocesses (and to qg ones in next-to-leading order in α_s). The gg initial state is expected to give the dominant corrections [14]. The authors of [15] estimate the resolved photon corrections to charm and bottom production to about 20%. The results, however, rely strongly on the not yet well known parametrizations of the parton structure functions in the photon. Experimentally a separation of heavy quark production through the direct mechanisms and the resolved photon processes seems to be feasible. Resolved photon contributions drop off rather quickly with increasing $p_\perp$. Also the rapidity distributions are different. Thus cuts in rapidity and $p_\perp$ (or even in Q^2) allow to isolate the resolved photon contributions from the direct BGF contributions to charm and bottom production. I note that there is potentially a problem of double counting. The splitting of the photon into collinear quark pair, Figure 6, is partially included in the contribution of the higher order QCD subprocess $\gamma + q \to Q + \bar{Q} + q$, see Figure 5. A cut in the $p_\perp$ of the $Q\bar{Q}$ system might allow a separation of the two contributions, but more work is needed for a clean separation.

A fair fraction of charm and bottom events is also expected in high energetic leptoproduction where the proton of the beam is scattered quasi-elastically with only very small energy loss and emerges at very small momentum transfer. Hard QCD scatterings in these diffractive reactions at HERA can be described by the exchange of a pomeron. Assuming that the pomeron can be characterized by a momentum density, $G_{\mathcal{P}}(x)$, describing gluons in the pomeron, the charm and bottom cross-sections at HERA in diffractive production were estimated [16] to $O(150\,\text{nb})$ for $c\bar{c}$ and $O(0.8\,\text{nb})$ for $b\bar{b}$. These cross-sections amount to about 10% of the total charm and bottom cross-sections.

Finally there are uncertainties particularly relevant for charm production. First there are higher twist effects, suppressed by a power of $1\,\text{GeV}/m_Q$, thus non negligible for charm production. A possible higher twist contribution is the concept of intrinsic charm [17] where one imagines that the heavy quark exists as part of the hadron wave function. Another possibility is the effect of coalescence enhancement [18] based on final state interactions of the heavy quark with the proton remnants. Secondly, there is the problem of considering the charm quark as a "parton". Evolved parton distributions containing the charm quark require a proper subtraction in the QCD corrections not to double count the contribution where the exchanged virtual quark is nearly on mass-shell and collinear to the incoming gluon [19].

For top production in ep collisions there exists still another source, namely the production of a $W^{\pm}$ boson which subsequently decays into $\bar{t}b$ (or $t\bar{b}$). The W production cross-section at HERA is estimated to be [20], $\sigma_W \sim 0.5$–1 pb, resulting in 5–10 top events per year ($\int Ldt = 200\,\mathrm{pb}^{-1}$). This corresponds to an increase of about 5–30% of the total top cross-section for $m_t = 50$–70 GeV and is thus a non negligible contribution in that mass range.

4 Characteristics of heavy flavour production *ep* collisions

Having found that the production of heavy quarks is dominated by BGF I now study their characteristics based on this mechansim. The basic features of heavy quark production can be derived from the lowest order formula. Since the full $O(\alpha_s^2)$ calculation of differential heavy quark distributions is still outstanding I account for the higher order effects on the event shape by the use of a parton cascade simulation algorithm [21] incorporated in the Monte Carlo event generator [11] which was used to obtain the following differential distributions. In this programme also the full hadronic final state is simulated including the target remnants [22] using the Lund string model [23] for the hadronization step.

I first discuss the overall kinematics specified by x, y and $Q^2 = xys$. A light top quark ($m_t \leq 40$ GeV) and also charm and bottom quarks are mainly photoproduced, i.e. we find the typical $1/Q^2$ behaviour with an exceedingly small lower limit in Q^2, $\sim m_e^2(4m^2/s)^2$, which, however, increases with the quark mass. Equivalently, the scattered electron is dominantly at very small angles and thus very hard to measure. Hence the kinematics must be reconstructed from the hadronic system. The Weizsäcker-Williams approximation can be used as a reasonable approximation [2], but let me emphasize that still about 1.7% of charm, 5% of bottom and 23% of top events are deep inelastically produced with $Q^2 \geq 10\,\mathrm{GeV}^2$. As a reflection of the Q^2 dependence the NC processes are also dominantly at small x. The cross-section is also peaked at small y for charm, but shifts to larger y with increasing mass through the increased threshold, $x_g ys \sim \hat{s} \geq 4m_Q^2$.

A heavy top quark ($m_t \geq 55$ GeV), on the other hand, is dominantly produced by the CC reaction (3). The exchange of the massive W boson leads to a rather uniform distribution in Q^2 and also in x and y. In fact, the Q^2 distribution of $\bar{t}b$ production is quite similar to the one of light quark production with a rather large mean value of Q.

The heavy quark antiquark system is specified by two of the following variables: The invariant mass of the $Q\bar{Q}'$ system, $\hat{s}$, the momentum fraction of the gluon, x_g, the transverse momentum of the heavy quark, $p_\perp$, and its rapidity, η, both measured in the $Q\bar{Q}'$ cms system or in the laboratory (Lab) frame (besides the azimuthal angle Φ, see eq. (4)). The distribution in the invariant mass of the $Q\bar{Q}$ system, $\hat{s}$, shown

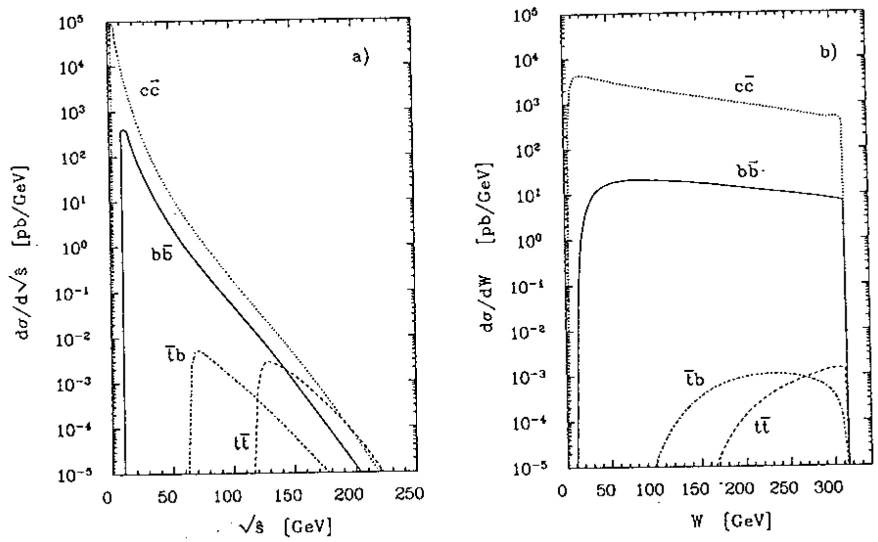

Figure 7: *Dependence of the BGF cross-section on (a) the invariant mass, $\sqrt{\hat{s}}$, of the heavy quark-antiquark system, and (b) the invariant mass, W, of the total hadronic system including the target remnant.*

in Figure 7a, dominates close to threshold and falls steeply above. The reason is the combined effect of the $1/\hat{s}^2$ dependence of the partonic cross-section and the strong fall-off of the gluon density with increasing x_g. The invariant mass W of the complete hadronic system, $W^2 = (1-x)Q^2/x$, has a rather different distribution, Figure 7b, due to the addition of the target remnant. A cut in W is not effective in separating the heavier flavours bottom and top from the dominant charm production whereas a cut in $\hat{s}$ would be better. On the other hand $\hat{s}$ is more difficult to measure experimentally.

Closely related to $\hat{s}$ is the momentum fraction, x_g, of the gluon, see eq. (5). From eq. (5) it is clear that both the lower limit on x_g and its mean value increase with the heavy quark mass. This is illustrated in Table 1. As was shown in [1] the x_g distributions of the heavy quark cross-sections follow closely the input gluon density which make an extraction of the gluon density at HERA feasible. From the experimental point of view, however, the variable x_g is not directly accessible and its reconstruction through eq. (5) depends on the ability to determine $\hat{s}$ and the possiblity to separate the BGF mechanism where the gluon density enters at the Born level from all other heavy quark production processes.

The $p_\perp$ and rapidity behaviour of the heavy quark cross-sections can be understood most easily in the $Q\bar{Q}$ cms (with the boson gluon axis defining the z-axis). I shall discuss the corresponding distributions in the Lab frame afterwards. Consider

	$c\bar{c}$	$b\bar{b}$	$\bar{t}b$	$t\bar{t}$
$< x_g >$	0.025	0.034	0.19	0.29
$x_{g,\text{min}}$	9×10^{-5}	1×10^{-3}	0.04	0.14
$< y >$	0.18	0.29	0.55	0.77
$< \beta_{\text{long}} >$	-0.58	-0.52	-0.81	-0.82
$< \eta_{cms}^{Lab} >$	-0.67	-0.58	-1.1	-1.2

Table 1: *Mean and minimum value of the momentum fraction of the gluon, x_g, and average values of the momentum fraction of the boson, y, the longitudinal velocity of the $Q\bar{Q}$ sytem w.r.t. the Lab-system, β_{long}, and the rapidity of the heavy quark in the Lab-sytem, η_{cms}^{Lab}.*

the NC lowest order BGF cross-section in the WWA:

$$\frac{d^3\sigma}{dydx_gdz} = P_\gamma(y)g(x_g,\mu_F^2)\frac{\text{const}}{yx_gs}\left[\frac{z}{1-z} + \frac{1-z}{z} + \frac{4m^2}{z(1-z)\hat{s}} - \left(\frac{2m^2}{z(1-z)\hat{s}}\right)^2\right] \quad (9)$$

Here $P_\gamma(y)$ is the probability of finding a photon in the electron. Let us assume that the parton number densities are constant,

$$yP_\gamma(y)x_gg(x_g,\mu_F^2) \approx \text{const.} \quad (10)$$

Then introducing the transverse mass square of the heavy quark in the $Q\bar{Q}$ cms

$$m_\perp^2 \equiv p_\perp^2 + m^2 = z(1-z)\hat{s} \quad (11)$$

I can rewrite the cross-section in the following way:

$$\sigma \approx \text{const}\ \ln\left(\frac{s}{4m^2}\right)dz\frac{dm_\perp^2}{m_\perp^4}\left[1 - 2z(1-z)\left(1 - \frac{2m^2}{m_\perp^2} + \frac{2m^4}{m_\perp^4}\right)\right] \quad (12)$$

The integration limits are $m^2 \leq m_\perp^2 \leq z(1-z)s$ and $z_- \leq z \leq z_+$ where $z_\pm = (1 \pm \beta_0)/2$, $\beta_0^2 = 1 - 4m^2/s$. From eq. (12) we conclude that the $p_\perp$ beahaviour of the heavy quark in the $Q\bar{Q}$ cms is given by:

$$\frac{d\sigma}{dp_\perp^2} \propto \frac{\sqrt{1 - 4m_\perp^2/s}}{m_\perp^4} \quad (13)$$

Thus, in the $Q\bar{Q}$ cms we expect, $< p_\perp > \approx m$, and a fall-off at large $p_\perp$ as $1/p_\perp^4$. To obtain the $p_\perp$ distribution in the Lab frame we need to know the transformation between the $Q\bar{Q}$ sytem and the Lab frame. The transverse momentum of the scattered lepton has to be balanced by the $Q\bar{Q}$ sytem. Its modulus is given by

$$p_\perp^{DIS} = \sqrt{(1-y)Q^2} \quad (14)$$

Hence for the low Q^2 NC events the $Q\bar{Q}$ system and the Lab frame are only connected via a longitudinal boost along the beam axis. Thus the $p_\perp$ distributions of the heavy quarks in both frames will look quite similar. I show the $p_\perp$ (w.r.t. the beam

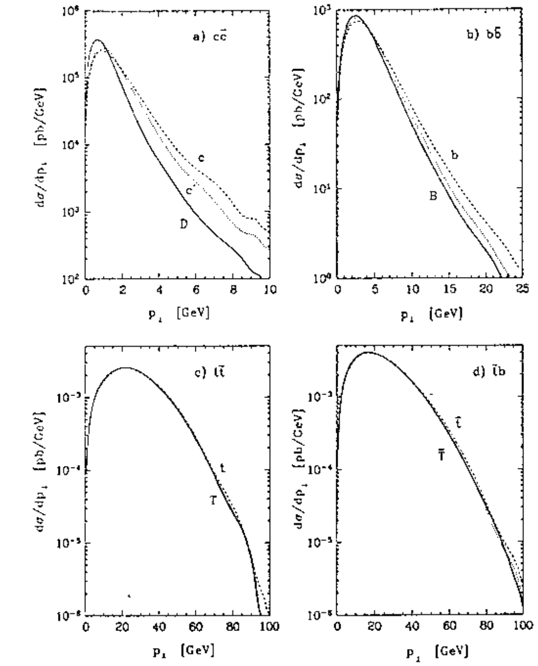

Figure 8: *Transverse momentum in the HERA lab frame for the heavy quark before (dashed) and after parton shower gluon emission (dotted), and for the corresponding hadrons after string fragmentation (full).*

axis) distributions of the heavy quarks in the HERA Lab frame in Figure 8. The distributions for NC heavy quark production indeed have the predicted characteristics with $< p_\perp > \approx m/2$. Only when $p_\perp \gg m_Q$, the curves are a bit steeper than the $1/p_\perp^4$ expected because the photon and gluon number densities $xf(x)$ are not constant, but decrease with increasing x. The effect of multiple gluon emission on the event shape can also be seen in Figure 8 as well as the distributions of the heavy hadrons. Their distributions essentially follow those of the corresponding heavy quarks.

The $p_\perp$ behaviour of the CC $\bar{t}b$ production cannot be explained in the foregoing way. Here Q^2 is typically so large that the $Q\bar{Q}$ cms and the Lab frame are no longer related by just a longitudinal boost. In fact, $< \sqrt{Q^2} >$ is larger than the $p_\perp$ of the hard scattering process, i.e. $< p_\perp^{DIS} > = O(Q)$ is larger than $< p_\perp^{QCD} > = O(m)$. Thus contrary to the NC production of light quarks, the $p_\perp$ of the heavy quarks in CC reactions is essentially given by the DIS $p_\perp$ eq. (14). This also explains why the $p_\perp$ distribution of $\bar{t}b$ events in Figure 8 is flater than the NC distributions.

I now come to the rapidity distributions of heavy quarks. In the $Q\bar{Q}$ cms the rapidity, η, is related to the variable z via (NC case):

$$\eta = \frac{1}{2}\ln\left(\frac{1-z}{z}\right) \quad (15)$$

Integrating eq. (12) over $m_\perp^2$ I find:

$$\frac{d\sigma}{d\eta} \propto \frac{e^{2\eta}+e^{-2\eta}}{(e^{\eta}(1+e^{2\eta}))^4} \qquad (16)$$

Thus in the $Q\bar{Q}$ cms we find that the rapidity distribution is central and approximatively constant for small values of η. Furthermore it falls off as the modulus of η becomes large.

The rapidity distribution in the Lab frame is given by:

$$\eta^{Lab} = \eta^{cms} + \eta^{Lab}_{cms} \qquad (17)$$

Here η^{Lab}_{cms} is the rapidity of the $Q\bar{Q}$ cms in the Lab frame. Its distributions can be understood once the distributions in x_g, y (and Q^2) are known. x_g, the momentum fraction of the gluon, is defined by the relation, $p = x_g P$, where p is the gluon and P the proton momentum. A similar relation can be found for the variable y. In the Lab frame we have:

$$y = \frac{E^\gamma + p^\gamma_{long}}{E^e + p^e_{long}} \qquad (18)$$

Here E^a and p^a_{long} are the energy and the longitudinal (along the beam axis) momentum of particle a in the Lab-system, respectively. Now, in the limit $Q^2 = 0$, eq. (18) simplifies to

$$q = y l_e \quad , \qquad (19)$$

i.e. the photon is emmitted collinearly from the electron moving along the beam axis. Thus for photoproduction the heavy quark cms and the Lab frame are related by a longitudinal boost only. The velocity of this boost is given by

$$\beta_{long} = \frac{yE^e - x_g E^p}{yE^e + x_g E^p} \qquad (20)$$

The rapidity, η^{Lab}_{cms}, entering eq. (17) can now be written as:

$$\eta^{Lab}_{cms} = \ln[\gamma(\beta+1)] = \frac{1}{2}\ln\left(\frac{yE^e}{x_g E^p}\right) \qquad (21)$$

For example at HERA, $E^e = 30\,\mathrm{GeV}$ and $E^p = 820\,\mathrm{GeV}$. Since the distributions of the cross-section in x_g and y are quite similar we expect the rapidity eq. (21) to be rather constant. In the limit $Q^2 \ll s, 4m^2 \ll s$, the variables x_g and y are limited symmetrically from below by the heavy quark mass, $yx_g \gtrsim 4m^2/s$, and their distributions are essentially independent of the heavy quark mass. Thus in the NC case the cms velocity and the cms rapidity should approximately be independent of the heavy quark mass. These ideas are confirmed in Table 1 where I give the average values of β_{long} and η^{Lab}_{cms}. Furthermore we observe that β_{long} and η^{Lab}_{cms} are quite small, i.e. the $Q\bar{Q}$ cms is almost at rest in the Lab frame, in mean it is slowly moving in the proton direction.

According to eq. (17) the rapidity of the heavy quark in the Lab frame is the sum of its rapidity in the $Q\bar{Q}$ cms and the rapidity of the latter in the Lab system. From the previous arguments we expect a broad distribution in η^{Lab} which is slightly shifted in proton direction. This behaviour can in fact be seen in Figure 9 where I show

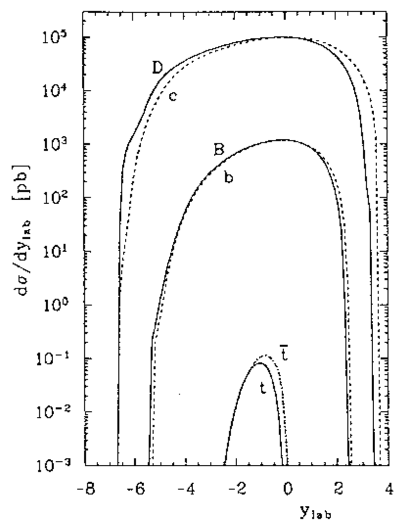

Figure 9: *Rapidity distribution of heavy quarks and hadrons (sum of mesons and baryons of the corresponding flavour) in the laboratory frame of HERA. The separate sets of curves are for $c\bar{c}$, $b\bar{b}$, $t\bar{t}$ and $\bar{t}b$ production, respectively. (Top quark and hadron curves overlap.)*

the rapidity distributions of the heavy quarks and hadrons in the Lab frame. Also shown are the distributions of the heavy hadrons fragmented with the LUND string fragmentation. Due to similar losses in both energy and momentum the rapidity is essentially unchanged by gluon radiation and fragmentation. We find that the asymmetric electron and proton momenta are thus almost completely compensated by a suitable choice of the photon and gluon energy fractions. It is only for top production that the heavy quark cms moves faster and thus the top quark is slightly more forward (in proton direction) produced in average. This can be explained by the fact that for top production such a high partonic energy $\hat{s}$ is needed that even with a maximum energetic photon ($y \to 1$) an even faster gluon is required.

I close this section by commenting the two modes of heavy quark production in ep collisions. NC heavy quark production in ep collisions is similar to the situation at the $p\bar{p}$ collider in the sense that the initial state of the hard scattering subprocesses consists out of two collinear partons. In ep collisions, the incoming electron with momentum l_e emitts collinearly a photon with momentum $q \approx yl_e$, and similarly the proton with momentum P a gluon with momentum $p = x_g P$, see Figure 10a. The scale μ of the whole process is thus set by the $p_\perp$ of the hard scattering subprocess which is of the order of the heavy quark mass:

$$\textit{low } Q^2 \textit{ events:} \qquad \mu \sim p_\perp^{QCD} = O(m_Q) \qquad (22)$$

Heavy top quark ($m_t \gtrsim 55\,\mathrm{GeV}$) events, on the other hand, are dominantly produced through the CC reaction (3). The Q^2 distribution of $\bar{t}b$ production is essentially

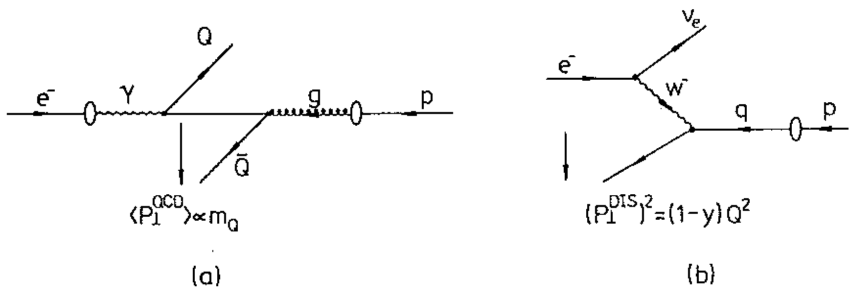

Figure 10: *The two modes of an ep collider: (a) low Q^2 events with a scale $\mu \sim p_\perp^{QCD}$, and (b) truely DIS events with $\mu \sim p_\perp^{DIS}$.*

the same as the one of light quark production with a rather large mean value of Q. Here the situation is complementary to the $p\bar{p}$ collider, the $p_\perp$ of scattered lepton which is balanced by the hadronic side sets the scale of the process rather independently of the quark mass, Figure 10b:

$$\textit{high } Q^2 \textit{ events:} \qquad \mu \sim p_\perp^{DIS} = O(\sqrt{Q^2}) \tag{23}$$

According to these two heavy quark production modes, charm and bottom signatures go along the lines of similar analyses in hadron collisions exploiting e.g. the $p_\perp$ of the lepton w.r.t. the beam axis [24]). In the contrary, a top search at HERA requires new strategies, in particular when investigating the nonleptonic top decay sample where the DIS CC background from light quarks is crucial [25].

Acknowledgements. I am grateful to G. Ingelman for interesting collaboration on this study. I thank A. Ali for organizing an interesting workshop and a pleasant stay in Erice.

References

[1] G. Ingelman and G.A. Schuler, Z. Phys. C40 (1988) 299.

[2] G.A. Schuler, Nucl. Phys. B299 (1988) 21.

[3] E. Eichten, I. Hinchliffe, K. Lane and C. Quigg, Rev. Mod. Phys. 56 (1984) 579, ibid. 58 (1986) 1047.

[4] A.D. Martin, R.G. Roberts and W.J. Stirling, Phys. Rev. D37 (1988) 1161.

[5] M. Glück, R.M. Godbole and E. Reya, Z. Phys. C38 (1988) 441.

[6] U. Baur and J.J. van der Bij, Nucl. Phys. B304 (1988) 451.

[7] M. Glück, E. Hoffman and E. Reya, Z. Phys. C13 (1982) 119.

[8] D.W. Duke and J.F. Owens, Phys. Rev. D30 (1984) 49.

[9] R.K. Ellis and P.Nason, FERMINLAB-Pub-88/54-T.

[10] G. Altarelli, M. Diemoz, G. Martinelli and P. Nason, Nucl. Phys. B308 (1988) 724.

[11] G. Ingelman and G.A. Schuler, AROMA 1.2 – A Generator of Heavy Flavour Events in ep Collisions, DESY preprint in preparation.

[12] P. Aurenche et al., Nucl. Phys. B286 (1987) 553.

[13] R.P. Feynman, Photon-hadron interactions, W.A. Benjamin Inc. 1972.

[14] R.K. Ellis and Z. Kunszt, Nucl. Phys. B303 (1988) 653.

[15] M. Drees and R. M. Godbole, MAD/PH/419 and DO-TH 88/13 preprint 1988.

[16] K. H. Streng, in Proceedings of the HERA Workshop, Hamburg 1987, Editor: R. D. Peccei.

[17] S. J. Brodsky, C. Person and N. Sakai, Phys. Rev. D23 (1981) 2745;
S. J. Brodsky, P. Hoyer, C. Person and N. Sakai, Phys. Lett. 93B (1980) 451.

[18] S. J. Brodsky, J. F. Gunion and D. E. Soper, Phys. Rev. D36 (1987) 2710.

[19] F. I. Olness and Wu-Ki Tung, Nucl. Phys. B308 (1988) 813.

[20] K. J. F. Gaemers et al., in Proceedings of the HERA Workshop, Hamburg 1987, Editor: R. D. Peccei.

[21] T. Sjöstrand and M. Bengtsson, Comput. Phys. Common. 43 (1987) 367.

[22] B. Andersson, G. Gustafson, G. Ingelman and T. Sjöstrand, Z. Phys. C13 (1982) 361.

[23] B. Andersson, G. Gustafson, G. Ingelman and T. Sjöstrand, Phys. Rep. 97 (1983) 31.

[24] A. Ali et al., in Proceedings of the HERA Workshop, Hamburg 1987, Editor: R. D. Peccei.

[25] G. Ingelman, G. A. Schuler and J. F. de Trocóniz, DESY 88-143 (1988).